

1 **Simulation-based approach to optimize passively designed buildings: a**
2 **case study on a typical architectural form in hot and humid climates**

3
4
5 Xi Chen*, Hongxing Yang and Weilong Zhang

6
7 Renewable Energy Research Group (RERG), Department of Building Services Engineering,
8 The Hong Kong Polytechnic University, Kowloon, Hong Kong, China

9
10 **Abstract**

11 Passive design strategies are important for achieving building sustainability given their proved
12 influences over the building performance in both energy and indoor environmental aspects. The
13 building layout, envelope thermophysics, building geometry and infiltration & air-tightness are
14 major passive architectural parameters to improve the building energy efficiency. In this paper, a
15 comprehensive literature review on simulation-based approaches to optimize passively designed
16 buildings is conducted and corresponding research gaps are identified. Based on existing research
17 methods, modelling experiments on a generic building are conducted to integrate robust variance-
18 based sensitivity analyses with an early-stage design optimization process. Proposed mixed-mode
19 ventilation and lighting dimming control algorithms are applied to the EnergyPlus model to
20 simulate the total lighting and cooling energy demands by incorporating the related design criteria
21 in a local green building assessment scheme. The non-dominated sorting genetic algorithm (NSGA-
22 II) is then coupled with the modelling experiment to obtain the Pareto frontier as well as the final
23 optimum solution. Different settings of NSGA-II are also investigated to improve the computational
24 efficiency without jeopardizing the optimization productivity. Furthermore, the sensitivity of
25 optimum design solutions to external environmental parameters in hot and humid areas are
26 explored. Findings from this study will guide decision-makers through a holistic optimization
27 process to fulfill energy-saving targets in a passively designed green building.

28 *Keywords: Passive design; green building; Optimization; Sensitivity analysis; NSGA-II*

29

* Corresponding author: Tel.:+852-2766 4726, Fax: 2765 7198, E-mail: climber027@gmail.com

30 **Contents**

1. Introduction.....2

2. Review of simulation-based passive design approach.....3

 2.1. Sensitivity analyses to identify important design factors.....3

 2.2. Optimization approach to improve building performance.....4

3. Research design and methodology.....6

 3.1. Selection of weather profiles.....7

 3.2. Determination of input variation and constraints.....8

 3.3. Definition of modelling algorithm and control setting.....9

 3.4. Variance-based sensitivity analysis.....12

 3.5. Multi-objective optimization and decision-making.....13

4. Case study on a prototype building.....14

 4.1. Initial sensitivity analysis.....14

 4.2. Preliminary optimization.....16

 4.3. Influence of different optimization setting.....17

 4.4. Optimum design configuration under different weather conditions.....18

5. Conclusions.....19

31

32 **1. Introduction**

33 Building sectors account for approximately 60% of the total energy use in Hong Kong
34 according to official statistics conducted by the local government [1]. Driven by the urge to reduce
35 the building energy demand and minimize its environmental impacts, local building design codes
36 (i.e. BEC 2015) and green building rating schemes (BEAM Plus Version 2.0) have been launched
37 recently to enhance the sustainable development of local communities. Among multiple building
38 design guidelines and assessment criteria, passive design is recently under the spotlight owing to its
39 proved effectiveness on improving the cooling and lighting performance of buildings [2, 3].
40 Because space cooling and lighting account for 41% of the total residential energy demand based on
41 statistics of the Electrical and Mechanical Services Department (EMSD) (as shown in Fig. 1) [4],
42 passive design features including the building layout, envelope thermophysics, building geometry
43 and infiltration & air-tightness can make great contributions to low energy or near zero energy
44 building designs [5]. Utilizing above passive strategies requires not only investigating their
45 individual impacts as presented in some existing research [6-8], but also incorporating a holistic

46 approach with deliberate consideration of interactive effects [9]. It is essential for architects and
47 engineers to understand the relative importance of each strategy and deploy them appropriately at
48 the first opportunity. Therefore, simulation-based optimization processes combined with in-depth
49 and exhaustive sensitivity analyses (SA) are thoroughly reviewed in this study and an exemplary
50 application of a proposed holistic design approach to a prototype high rise residential building in
51 hot and humid areas will be analyzed and discussed in detail.

52

53 **2. Review of simulation-based passive design approach**

54 **2.1.Sensitivity analyses to identify important design factors**

55 Multiples building design factors can be subject to extensive and systematic examinations by
56 different SA approaches using building simulation tools. According to Tian et al. [10], SA can be
57 categorized as the local sensitivity analysis and global sensitivity analysis. The local SA is used to
58 examine the impact of a certain input variable by independently changing its values while keeping
59 other variables fixed [11]. A commercial building in Hong Kong was subject to the local SA with
60 DOE-2 [12]. This study focused on the whole building design including the building structure,
61 geometry, occupancy, load condition and HVAC system. Important input factors for the building
62 annual energy use, peak load and load profile were identified respectively. A similar study was
63 conducted to explore optimal energy-saving solutions for high-rise residential building in
64 Netherland, where building envelope parameters such as the glazing type, window-to-wall ratio, sun
65 shading and roof strategies contributed to a total energy saving of 42% [13]. Samuelson at al.
66 performed a simple sensitivity analysis on the energy use intensity of case buildings in three urban
67 contexts, where the window to wall ratio, glazing type and building orientation are determined to be
68 the top three influential design factors [14]. Apart from investigating whole-building design inputs,
69 passive design was specifically examined to decide their importance for five major climatic zones in
70 China where retrofitting measures to improve the indoor thermal comfort and energy-saving
71 performance for each zone were identified respectively [15]. The window opening size was also
72 individually correlated with the peak load and annual energy consumption to provide concise design
73 charts for early planning stages [16]. In addition, a few similar studies looked into the thermal load
74 reduction efficiency by adjusting a single design variable such as the shape coefficient, envelope

75 thermal resistance or occupant behavior pattern [17, 18]. Instead of modulating one design factor at
76 a time in building simulations, the global SA can study building performances with the regression
77 (i.e. sampling-based), screening-based or variance-based methods [19, 20]. The uncertainty and
78 sensitivity of the indoor thermal comfort condition in a passively cooled office were examined by
79 regression analyses [21]. According to the findings, the indoor weighted temperature excess hours
80 (WTE) was most sensitive to the single-sided ventilation. Yildiz and Arsan estimated the impact of
81 design parameters of low-rise apartment buildings in hot and humid climates using regression
82 analyses coupled with the Latin Hypercube Sampling (LHS) and Monte Carlo approach [22], where
83 the window size, U-value and solar heat gain coefficient (SHGC) were proved to have the greatest
84 impact on heating and cooling loads of different floors. The Morris method (i.e. a popular
85 screening-based method), which enables a qualitative assessment of the influence from each design
86 variable, was integrated into a multi-criteria decision-making process for minimizing energy
87 consumption and degree-hours of residential buildings in Brazil [23]. The most influential envelope
88 feature in each climate zone was filtered out as further inputs to the performance evaluation of
89 construction systems. The Analysis of Variance method (i.e. variance-based) was deployed in an
90 uncertainty and sensitivity prediction of available solar irradiation on exterior building surfaces with
91 shading devices [24]. The building latitude, orientation and width of overhang fins were proved to
92 have more influence over calculated solar fractions and the uncertainty quantification process was
93 identified as a crucial prerequisite for maintaining the building energy balance.

94

95 **2.2.Optimization approach to improve building performance**

96 Based on identified influential design variables from sensitivity analyses, a design optimization
97 can be further conducted to improve the life-cycle cost effectiveness, energy efficiency and indoor
98 environment qualities of buildings. Optimization studies can usually be classified to the mono-
99 objective optimization and multi-objective optimization, where the latter is more common in
100 building research area considering the requirements from multi-criteria design guidelines and
101 assessment schemes [25-27]. Carlucci et al. carried out a four-objective optimization of a detached
102 zero-carbon house in Italy and discussed trade-offs between the thermal and visual discomfort [28].
103 Futrell et al. performed both the pattern search and meta-heuristic optimization with GenOpt to

104 simultaneously minimize the cooling, heating and lighting energy demand [29]. The target building
105 was optimized respectively for each orientation and conflicts between thermal and daylight
106 objectives were observed. In a similar work, energy performance optimization with the Multi-island
107 Genetic Algorithm (GA) was performed on a software platform developed with the QT language
108 and OpenGL interface [30]. When miscellaneous daylight illuminance indices were treated as
109 optimization objectives, the window characteristics, building orientation and wall reflectance were
110 thoroughly explored by evolutionary algorithms to search for an optimum interior design [31]. Final
111 solutions were determined by their appearance frequencies in 6 sets of Pareto frontiers together with
112 their mean distances to utopia points. As a holistic building design approach in early stages, multi-
113 objective optimizations were also conducted with the energy use, thermal comfort and capital cost
114 as objectives [32-34]. On top of abovementioned optimization objectives, Zhang et al. investigated
115 trade-offs between the obtained solar radiation, space efficiency and shape coefficient of free-form
116 buildings by changing building geometry inputs with Rhinoceros and Grasshopper [35]. In addition,
117 the multi-objective particle swarm optimization (MOPSO) algorithm was exploited instead of GA
118 methods to search for Pareto optimal solutions for a generic room model under different weather
119 conditions of Iran [36]. Ruiz et al. proposed a methodology to accurately perform the automated
120 building envelope calibration under the International Performance Measurement and Verification
121 Protocol (IPMVP). A reliable energy simulation model was obtained from the Non-dominated
122 Sorting Genetic Algorithm-II (NSGA-II). Furthermore, building orientations and window
123 characteristics were optimized by comparing the performance of the Hooke-Jeeves Algorithm,
124 Multi-objective Genetic Algorithm-II and Multi-objective Particle Swarm Optimization Algorithm
125 in terms of the stability, robustness, validity, speed, coverage and locality [37].

126 According to the above brief introduction and in-depth literature review (summarized in Table
127 2), it can be recognized that there is little research in combined sensitivity and optimization analyses
128 of passively designed buildings in hot and humid climates under hybrid ventilation conditions. This
129 paper mainly focuses on the energy demand minimization of a generic building model with selected
130 significant input design variables based on a comprehensive sensitivity analysis. Simulation models
131 with designed mix-mode ventilation and light dimming control strategies were coupled with
132 NSGA-II to obtain the Pareto frontier as well as the final optimum solution under different

133 algorithm settings and weather conditions. The originality of this article lies in the following points:
134 (1) This optimization study is incorporated with sensitivity analyses to screen out the most
135 significant influential factors and is therefore capable of improving the efficiency of optimization
136 algorithm; (2) In most existing studies, only limited types of windows or walls are investigated,
137 whereas this research thoroughly explores the whole feasible range of various thermal and lighting
138 properties of passive design elements with a robust global sensitivity analysis; (3) External
139 obstructions are usually overlooked by reviewed studies, which are proved to be a significant design
140 factor and crucial in green building assessment with at least five relevant criteria specified in
141 BEAM Plus; (4) The holistic design approach in this study is highly incorporated with the existing
142 green building rating scheme, and the synergy of energy and indoor environment aspects are
143 carefully considered in the decision making process; (5) Thermal comfort performance no longer
144 contradicts with energy saving targets as observed in many existing multi-objective optimizations
145 because of the application of adaptive thermal comfort model in the building performance
146 simulation and assessment; (6) Monthly variation of sensitivity indices is investigated instead of
147 short-term (i.e. daily or hourly) uncertainty profiles as presented in existing literatures and most
148 suitable optimization settings specific to the proposed optimization problem is obtained; (7) The
149 sensitivity analysis of optimization settings provided a more precise algorithm configuration
150 compared with using empirical values suggested by existing literatures.

151

152 **3. Research design and methodology**

153 This study focuses on a simulation-based approach to optimize the energy efficiency of passive
154 designed buildings under hybrid ventilation and lighting dimming conditions by deliberately
155 considering the daylight and thermal comfort requirements in local green building guidelines (i.e.
156 BEAM Plus). Based on previous statistical modeling studies [38, 39], a generic building model has
157 been developed with determined probability distributions of architectural design parameters.
158 Control algorithms of the hybrid ventilation, daylight and thermal comfort are designed and
159 specified referring to local or international building standards. With a sufficient number of
160 modelling samples, the variance-based sensitivity analysis is performed to address the interaction
161 and non-linearity of input variables. The obtained sensitivity indices and their seasonal profiles can

162 help refine the problem space for the consequent optimization process by identifying high impact
163 design factors. The Non-dominated Sorting Genetic Algorithm-II (NSGA-II) is then adopted to
164 simultaneously minimize the cooling and lighting energy demand and obtain the Pareto frontier,
165 where the final optimum solution was derived from the weighted sum approach. Optimization
166 control parameters were also adjusted to improve the computation efficiency while maintaining the
167 productivity of the algorithm. The whole research process is summarized in Fig. 2.

168

169 **3.1. Selection of weather profiles**

170 Meteorological data in hot and humid subtropical or tropical climatic zones are selected as
171 weather inputs for building performance assessment during the cooling period, and Hong Kong
172 (22.3 N°, 114.17 E°) is therefore chosen as a benchmark for the case study. The TMY2 data of Hong
173 Kong is presented in Fig. 3 [38], which is considered a good approach to conduct building
174 simulations. The annual average dry bulb temperature and relative humidity of Hong Kong are
175 23.1 °C and 78.1 %, and the use of air-conditioning usually lasts from April to October based on
176 recommendations from BEAM Plus [40]. However, April is excluded from the simulation when the
177 ASHRAE55 adaptive comfort model with 90% acceptability is used to assess thermal comfort
178 conditions based on recommendations in previous research [41-43].

179 Apart from Hong Kong, four large metropolises characterized by high temperature and relative
180 humidity as well as rich solar and wind resources are selected to exam the sensitivity of optimal
181 solutions to external environmental parameters. Their climatic and geographic situations are briefly
182 summarized in Table 1. Bangkok (BKK) has the highest seasonal average temperature (29.12 °C)
183 and solar radiation (147.77 kWh/m²) but the lowest mean relative humidity (74.43%) in the whole
184 cooling season. Hong Kong (HK), Guangzhou (GZ) and Taipei (TPE) are all influenced by the
185 adjacent mainland and thus exhibit similar trends in the temperature and relative humidity. The
186 solar-wind conditions of TPE and HK are subject to impacts of strong tropical cyclones where the
187 highest monthly wind speed occurs at the end of the cooling season. The average radiation level of
188 GZ (103.17 kWh/m²) was the lowest in five cities because of the slightly higher latitude. Above
189 climate indices in Singapore (SGP) are however comparatively stable with the lowest average wind
190 speed of 1.92 m/s and the highest average relatively humidity of 82.63%. Overall, all five cities

191 have great potential for the application of passive design strategies, which can significantly reduce
192 the building energy demand.

193

194 **3.2.Determination of input variation and constraints**

195 3.2.1. Building Layout

196 The building layout includes the external obstruction angle (EOA) and building orientation
197 (BO). BO is altered in the modelling experiment from 0 to 360 degrees to assess its influence when
198 windows are only located on a single facade of the building. EOA measures the external shading
199 effects from a street canyon which is a common situation in large metropolis with high population
200 densities. The length of external obstruction is fixed to 100 meters as suggested in existing
201 literatures [44-46]. The distance and height of external obstructions are basic elements for
202 calculating EOA, which is defined as the angle between the horizontal line at the window sill level
203 and the line connected with the highest point of the external obstruction [40, 47, 48]. The EOA
204 should vary between 0° (i.e. unobstructed condition) to 87° with the assumption that the average
205 obstruction height is 100 m and the minimum separation from the obstruction (i.e. road width) is 5
206 m [49].

207 3.2.2. Envelope thermophysics

208 The envelope thermophysics is referring to the external wall thermal resistance (WTR),
209 specific heat (WSH), window U-values (WU) and solar heat gain coefficient (SHGC). The wall
210 thermal resistance changes from a baseline equivalent thermal resistance of $0.09 \text{ m}^2 \text{ K/W}$ (0.005 m
211 mosaic tiles + 0.01 m cement/sand plastering + 0.1 m heavy concrete + 0.01 m gypsum plastering
212 [50]) to a highly insulated one of $10.56 \text{ m}^2 \text{ K/W}$ as suggested by the 2009 ASHRAE Handbook-
213 Fundamentals. The wall specific heat changes from 800 to 2000 J/kg K as default limit values in
214 EnergyPlus modelling guidelines [51, 52]. The window thermal properties changes from a triple-
215 vacuum low emissive glazing (i.e. SHGC=0.1 and U-value= $0.2 \text{ W/m}^2 \text{ K}$ [53]) to a clear single
216 glazing (i.e. SHGC=0.9 and U-value= $6.0 \text{ W/m}^2 \text{ K}$). The window light to solar gain ratio is fixed to
217 one in the modelling experiments to represent a traditional low-e glazing. The covariation of the
218 visible light transmittance (VLT) and SHGC might cause conflicts between daylight and thermal
219 performances.

220 3.2.3. Building geometry

221 The building geometry involves the window to ground ratio (WGR) and overhang projection
222 fraction (OPF). The window to ground ratio changes between 10% and 50% based on the limitation
223 of external wall areas as well as mandatory window opening requirements in the local building
224 ordinance. On the other side, the overhang project ratio is subject to an upper limitation of 0.56 so
225 that the total overhang length would not exceed 1.5 m so that its projection area will be exempted
226 from the plot ratio and site coverage calculation.

227 3.2.4. Infiltration & air-tightness

228 The infiltration & air-tightness is evaluated by the infiltration air mass flowrate coefficient
229 (IAMFC) of the crack on the external wall surface. IAMFC stands for the air mass flow rate under
230 reference test conditions and varies between 0.01 and 0.03 kg/s in the simulation. The upper limit
231 prevents the air change rate from exceeding 1.5 ACH which should be a level of induced natural
232 ventilation rather than uncontrolled infiltration. The lower limit is a typical value of infiltration for
233 the room to reach an air change rate around 0.5 ACH as specified in the Building Energy Code.

234 The abovementioned input variables are uniformly sampled as non-informative distributions to
235 evaluate their relative impacts on the building energy efficiency [54]. In addition, building surface
236 properties (e.g. the solar absorptance and reflectance of external and internal building surfaces) are
237 preset with reasonable assumptions and excluded from sensitivity analyses because their
238 information can only be confirmed in later construction stages [48, 55, 56].

239

240 **3.3. Definition of modelling algorithm and control setting**

241 3.3.1. Description of the building modelling

242 A generic building model is prototyped to represent a typical high-rise building (usually 30 to
243 40 floors) developed by the Hong Kong Housing Authority which accommodates over 30% of the
244 local population [57]. These buildings are modularly designed with a standard floor layout plan as
245 shown in Fig. 4 [58]. A two-habitant hypothetical generic model in the center of the typical floor with
246 window openings on a single heat transfer facade surrounded by adiabatic surfaces is constructed to
247 represent the worst-case scenario for the daylight and ventilation access [38]. The space is assumed
248 to be occupied by two people with average activity levels of 100 W/person (between seated and

249 sleeping). The lighting and equipment load are set to be 15 W/m² and 142 W/Room referring to the
250 BEAM Plus guideline and Building Energy Code, based on which building operation schedules
251 including the cooling, lighting, equipment and occupancy are specified in Fig. 5, to represent a
252 combination of space functions of living room and bedroom [50].

253 The cooling and lighting energy demand is derived from interlinked sub-modules in
254 EnergyPlus, which has been extensively recognized, calibrated and validated in building
255 performance analyses [59, 60].

256 The daylight illuminance level on the specified indoor reference point is first derived from the
257 external available solar illuminance, window transmittance, room geometry and surface properties
258 [52]. Consequently, the artificial lighting is modelled to meet the a threshold of 150 Lux as
259 recommended by CIBSE Code of Lighting at the reference point [61]. The required fractional
260 lighting output with respect to its full load occasion is calculated according to the “continuous/off
261 dimming control” method [62].

262 The airflow network (AFN) model calculates multi-zone airflows driven by the outdoor wind
263 pressure and stack effect through cracks and window openings. It is used to simulate the single-
264 sided mixed-mode ventilation with the HVAC system as the supplementary solution. In an AFN
265 model, the airflow is induced by the pressure difference between air paths and zones. The model
266 further derives node temperatures and humidity ratios from the airflow rate and decide zone thermal
267 loads, where air balance equations are applied and corresponding zone air conditions are obtained
268 [43].

269 The IdealLoadsAirSystem is chosen to maintain the indoor thermal comfort condition when
270 natural ventilation alone cannot meet the requirement. The module is a simplified HVAC
271 component to calculate the cooling energy demand without handling too much details of the whole
272 system design. The module can emulate an ideal unit which mixes air at the zone exhaust condition
273 and removes the cooling load at 100% efficiency. The single cooling setpoint controller is used as
274 the HVAC system thermostat to comply with the upper limit of the ASHRAE55 adaptive comfort
275 model, which varies monthly with the prevailing outdoor air temperature [63].

276 The whole simulation model under naturally ventilated unoccupied conditions has been
277 partially validated by an on-site measurement of selected flats in a local Public Rental Housing

278 development, where the indoor temperature, relative humidity, air change rate and daylight factor
279 showed reasonable trends [40].

280 3.3.2. Hybrid ventilation control and comfort index

281 Control of hybrid ventilation is proposed in this research to maximize the benefit of deploying
282 passive design strategies. Silva et al. adopted a hybrid ventilation control method by allowing
283 natural ventilation only during daytime while set on the air-conditioners at night [23]. However, a
284 previous study performed by the authors consolidated that a full-day ventilation can lead to better
285 building performance compared with daytime or nighttime ventilation approaches [40]. Therefore,
286 the hybrid ventilation is allowable throughout the whole cooling period in this simulation. Although
287 an existing study claims that EnergyPlus does not permit the co-operation of HVAC and Airflow
288 Network (AFN) modules and the integration has to be realized by programming with Energy
289 Management System (EMS) [64], yet the hybrid ventilation is actually feasible by introducing the
290 Hybrid Ventilation Availability Manager.

291 The hybrid ventilation availability manager is applicable to spaces void of HVAC air loops.
292 The controller serves as a preventer of simultaneous natural ventilation and mechanical cooling and
293 is aimed to reduce the space cooling load by examining various strategies to maximize natural
294 ventilation. The controller starts operating at the beginning of each timestep and can override local
295 controls of both HVAC and AFN. It first checks the outdoor dry-bulb temperature when the
296 “Temperature” mode is selected for the ventilation mode control schedule. If the temperature is
297 within the preset upper and lower limits, the natural ventilation is possible. Then the indoor
298 operative temperature is compared with the 90% acceptability upper limits of the adaptive comfort
299 model which depend on the changing monthly mean outdoor temperature (calculated as 28.4, 28.9,
300 29.1, 28.8 and 28.1 °C from May to October as shown in Fig. 6) [65]. Assessing thermal comfort in
301 naturally ventilated or mix-mode buildings with adaptive model is appropriate and viable because
302 of the existence of occupant control and the psychological shift of expectations which cannot be
303 addressed by traditional heat-balance based models [66-68]. Once the indoor operative temperature
304 is lower than the calculated upper limits for each month, the natural ventilation will be executed
305 whenever the outdoor temperature is lower. Otherwise the window should be closed and the HVAC
306 system is then operated according to the availability status indicated by the cooling schedule. The

307 above control circuit is summarized in Fig. 7.

308

309 3.4.Variance-based sensitivity analysis

310 The variance-based method is chosen to conduct the initial sensitivity analysis for the
311 subsequent optimization because it is not limited by the model format and suitable for either non-
312 linear or non-additive models [69]. The total variance of the output $V(Y)$ is decomposed into
313 conditional variances of increasing dimensionality as shown in Eq. (1) [70].

$$314 \quad V(Y) = \sum_{i=1}^k V_i + \sum_{j>i}^k V_{ij} \cdots + V_{12\cdots k} \quad (1)$$

315 where $\sum_i^k V_i$ is the sum of conditional variances for the main effect of each input parameter; $\sum_{j>i}^k V_{ij}$
316 includes all conditional variances of the interaction between two input parameters; and $V_{12\cdots k}$ stands
317 for the conditional variance including the interaction of all inputs.

318 If the above equation is divided by $V(Y)$, the relationship between different orders of
319 sensitivity indices can be obtained:

$$320 \quad 1 = \sum_{i=1}^k S_i + \sum_{j>i}^k S_{ij} + \cdots + S_{12\cdots k} \quad (2)$$

321 where the S_i is called the first-order sensitivity index, which stands for the independent impact of X_i
322 on the variance of Y . It is defined to be the average conditional variance left when X is frozen to all
323 possible values in the probability density function (See Eq. (3)) [71].

$$324 \quad S_i = \frac{V_{X_i}(E_{X_{-i}}(Y | X_i))}{V(Y)} \quad (3)$$

325 Apart from the main effect of each input expressed by S_i , S_{ij} stands for the part of responses
326 of Y to the change of X_i and X_j which cannot be explained by the superposition of S_i and S_j . This
327 interaction effect between X_i and X_j is called the second-order sensitivity index. Similarly, there
328 might be a fraction of output impact which cannot be explained by the summary of all lower order
329 indices, taking the form of the higher-order index $S_{12\cdots k}$ [54].

330 Among different orders of indices, the first-order index is usually linked to “Factor
 331 Prioritization”, where the input with the highest S_i is deemed as the most influential factor.
 332 However, an input parameter should not be excluded from further analyses solely based on its first-
 333 order index, because the input might be involved in a relation of higher orders. Therefore, Eq. (4)
 334 calculates a total sensitivity index S_{Ti} summarizing the all orders of indices to identify an
 335 insignificant factor. If S_{Ti} is zero, then the input can be fixed at any possible value [72]. In this
 336 regard, the total sensitivity index can be used for “Factor Fixing” to prune the model input space for
 337 optimization problems. The Extended FAST model is used as the Analysis of Variance (ANOVA)
 338 method in this research to screen out influential passive strategies given its higher computation
 339 efficiency than the Sobol model [73].

$$340 \quad S_{Ti} = S_i + \sum_{j \neq i}^k S_{ij} + \dots + S_{i \dots j \dots k} \quad (4)$$

341

342 **3.5. Multi-objective optimization and decision-making**

343 As mentioned in previous sections, the lighting and cooling energy demand are chosen to
 344 compose optimization objectives which can indicate the influence of efficient passive designs. In
 345 order to solve the multi-objective optimization problem, the non-dominated sorting genetic
 346 algorithm II (NSGA-II), which is characterized by the higher computation efficiency, enhanced
 347 probability to create better solutions, and maintained population diversity by the crowding
 348 comparison, is applied to crucial design factors identified by the initial SA study [74]. The NSGA-II
 349 is chosen for this research because of its wide application and smooth integration with EnergyPlus
 350 [36, 75]. The algorithm introduced the concept of elitism which combines a parent population and a
 351 child population to reproduce the next parent generation based on the non-domination ranking
 352 method. If the number of non-dominated solutions exceeds the preset population size, it will be
 353 decreased according to the crowding distance measure [76].

354 In general, the population size, number of generations, crossover and mutation probability are
 355 required to setup an optimization process. The population size is suggested to be twice the number
 356 of input variables, and up to 1800 evaluations are usually necessary to enable the convergence [76].
 357 Furthermore, the crossover and mutation probability are preset to 0.9 and 0.355 respectively with

358 reference to a statistical analysis of 68 optimization studies [28]. However, these settings are subject
359 to an adaptive variation in this study to find the most suitable configuration.

360 When the NSGA-II program converges within the preset generations, non-dominated solutions
361 are sorted out as the Pareto frontiers, where one solution has equal prevalence over all the others
362 [77]. In order to obtain a single optimal solution, the weighted sum method is adopted to turn the
363 partial order into a total order on the objective space [78]. In this case, weightings for both lighting
364 and cooling energy demands are equal, making the total energy demand an ultimate optimization
365 target.

366

367 **4. Case study on a prototype building**

368 A typical high-rise residential building in Hong Kong was used to perform the case study in
369 this simulation-based optimization approach. Initial sensitivity analyses with time-series results
370 helped exclude insignificant design factors to improve the optimization efficiency, while NSGA-II
371 was performed to obtain the final optimum solution in the early design stage under different
372 algorithm settings and weather conditions in hot and humid areas. Major findings and discussions
373 with reference to existing studies are presented in this section.

374

375 **4.1. Initial sensitivity analysis**

376 The Analysis of Variance (ANOVA) with the FAST method managed to decompose the
377 uncertainty of the annual energy demand (i.e. cooling and lighting) in response to the defined
378 variation of design factors. This analysis totally involved 5632 simulations, which cost dramatically
379 more computation time compared with a previous regression-based approach [38]. Fig. 8 shows that
380 the window transmittance (SHGC/VLT) is the most prioritized input in all passive design strategies,
381 behind which the external obstruction height (EOH) and external obstruction distance (EOD) are
382 ranked in view of their influences over the total energy demand. This result also echoes with
383 findings by regression analyses in previous works [62, 79]. However, BO, whose impact was almost
384 ignorable judged by its regression coefficient, is ranked fourth in this analysis. WTR, WSH and
385 IAMFC all make no unique contribution to the output with zero first-order indices. The
386 inconsistency between the variance-based and regression analyses might result from the non-

387 additive building model as indicated by the subtotal of first-order indices (i.e. 0.670) less than one.
388 The remaining 33% of uncertainties in the output is then attributed to interactions between different
389 design factors.

390 Subsequently, total-order sensitivity indices are calculated and compared to first-order indices
391 in Fig. 9. Most total-order indices are larger than their first-order counterparts due to additive
392 interactions of different orders. Their rankings generally agree well with first-order counterparts
393 except that the window to ground ratio (WGR) becomes the third influential factor among all
394 inputs, surpassing the building orientation (BO), overhang projection ratio (OPF) and EOH. The
395 sum of total-order indices is 1.343, which can explain all variances in the total energy demand. In
396 addition, sensitivity indices of the infiltration air mass flow coefficient (IAMFC) and wall specific
397 heat (WSH) still equal zero and are consequently excluded from the optimization problem space.
398 Although WTR has no unique contribution to the output, yet it is proved to have a certain
399 interactive impact with other inputs and thus included for further optimization studies.

400 Furthermore, monthly variance-based sensitivity indices are shown in Fig. 10 to illustrate the
401 seasonal variation of design impacts. This information is important to estimate the interference of
402 outdoor ambient conditions, but is only available for short time periods in existing SA studies [24,
403 72]. Kristensen et al. conducted a time series estimation for elementary effects of envelope factors
404 and air-conditioning setpoints, whereas their simulation results cannot clearly present the variation
405 of Morris sensitivity indices [80]. In this regard, Fig. 10 gives a detailed illustration of monthly
406 sensitivities of the cooling, lighting and total energy output to each passive design strategy.

407 As shown in the sensitivity variation for the lighting output, there is a noticeable increasing
408 trend of SHGC/VLT and EOD starting from August, accompanied by corresponding decreases of
409 other influential design factors such as EOH. This time series variation can be explained by the
410 available solar radiation. In Hong Kong, the solar radiation level peaks in July, while the solar
411 altitude starts to drop after the summer solstice. Consequently, the solar irradiance in lower angles
412 can bypass the overhang projection and fall on the window surface. This condition has made the
413 lighting energy demand more sensitive to the window transmittance and obstruction distance. The
414 same reason caused the dramatically increased sensitivity index of BO, when the difference
415 between the available solar radiation on north and south facing building facades grows with the
416 subsolar point moving towards the southern hemisphere.

417 On the other side, the variation of sensitivity indices for the cooling energy output follows the
418 trend of outdoor dry bulb temperature as presented in Fig. 3. However, the substantial increment of
419 the sensitivity index of BO in October can also be attributed to the increased availability of the solar

420 radiation on building facades. In addition, the seasonal change of sensitivity indices for the total
421 energy demand is more similar to that for the cooling energy output, because cooling accounts for
422 larger building energy demand than lighting.

423

424 **4.2.Preliminary optimization**

425 From the above sensitivity analysis, eight design factors are selected to compose the
426 parametric problem space by a uniform sampling from their distribution ranges. Based on the
427 simulation setting specified in Section 3, totally 3124 evaluations were made before the
428 optimization engine reached the convergence.

429 As a result, 108 sets of Pareto optimal solutions are identified from the design problem space
430 as highlighted in Fig. 11. The Pareto Frontier conspicuously exhibits a trade-off conflict where the
431 cooling energy demand increased as the lighting energy demand decreased. The annual lighting
432 energy varies slightly from 13.30 kWh/m² to 14.70 kWh/m², while the cooling energy changes
433 dramatically from 21.04 kWh/m² to 77.60 kWh/m². In this simulation, minimizing the cooling
434 energy is equivalent to maximizing the thermal comfort, as the cooling thermostat setting is based
435 on temperature fluctuation ranges within the comfort zone. It is an approach different from most
436 existing optimization research where the thermal comfort and air-conditioning energy objectives
437 conflict with each other [33, 81]. Part of the conflict between minimizing the cooling and lighting
438 energy demand is attributed to the fixed light to solar gain ratio, where less solar heat gain incurs
439 less daylight access. If a selective window film, which filters thermal radiation while keeps high
440 transparency, is included in the passive design, the conflict can be alleviated to a certain extent.
441 Nonetheless, WGR, OPF and EOA still cause the converse effect on cooling and lighting energy
442 outputs. Since the Pareto optimization only imposes a partial order on solution candidates, a total-
443 order based fitness assignment can be suitable for external decision-making to obtain the final
444 single solution [78]. The weighted sum method is a linear aggregation of objective functions
445 multiplied by importance indicators or weightings, which are set to be equal in this study. The bi-
446 objective problem is then reduced to a mono-objective one which can be solved by NSGA-II with
447 the same setting. The ultimate solution was found to be 35.73 kWh/m², with a breakdown of 14.66
448 kWh/m² electric lighting and 21.07 kWh/m² mechanical cooling demand. The optimum solution is
449 attributed to a high window U-value and window to ground ratio of 5.81 and 0.49 W/m² K, a low

450 window transmittance and wall thermal resistance of 0.11 and 0.26 m² K/W, as well as a small
451 shading projection ratio of 0.15. All glazing of the optimum design is facing north and less shaded
452 by surroundings with an EOA of 14.00°. The solution is different from previously conducted
453 optimization of the same building in natural ventilation conditions [38]. Such difference can be
454 caused by the adopted hybrid control algorithm and building operation schedules.

455

456 **4.3. Influence of different optimization settings**

457 As per previous introduction, settings for the above preliminary optimization referred to
458 statistical analyses of existing building optimization research. As a rule of thumb, the crossover
459 probability usually assumes a higher value to allow swift exploration of the entire search space,
460 while the mutation rate is kept lower to control the convergence speed within a reasonable range
461 [82, 83]. These general guides are obtained from empirical studies, whereas the most appropriate
462 setting of NSGA-II might depend on practical scenarios, so that the previous optimization setting is
463 subject to examination in this section to consolidate its viability in terms of the solution quality and
464 computation efficiency. Below modelling cases are all conducted to achieve a weighted single
465 objective (i.e. the total building energy demand).

466 Fig. 12 illustrates the change of optimization progress when the population size is reduced
467 from 32 to 4, which explored a broader range compared to a related optimization study on
468 residential buildings [84]. All optimization tests managed to achieve convergence within 100
469 generations, when the total number of evaluations dropped from 2955 to 361. However, the
470 minimum total energy demand of 35.50kWh/m² can only be obtained when the population size is
471 equal or larger than 16, which can provide required number of evaluations indicated in existing
472 literatures [76]. Therefore, the following parametric tests on the crossover and mutation probability
473 are based on a reduced population size of 16 instead of 32 used for preliminary analyses.

474 Crossover is a reproduction method in genetic algorithms to create new individuals for the
475 next-generation population. It is a recombination of genes from parental generations and thus
476 recognized as a binary search operation. When the crossover rate is tuned down from 1.0 to 0.0, Fig.
477 13 showed that the required generations for arriving at a global optimal solution decreased from 98
478 to 50. Despite the increased convergence speed, the optimum solution can only be attainable when

479 the probability is no less than 0.8 compared with the preliminary optimization analysis. Although
480 conducting search operations with fewer crossovers can greatly save computation efforts, yet the
481 search engine can be stuck with local optimal solutions without exploring the whole design problem
482 space.

483 Mutation in the genetic algorithm is referring to the small and random variation in the
484 genotype [78]. It is another method of reproduction in optimization search operations. As presented
485 in Fig. 14, the convergence cannot be researched within the specified 100 generations when the
486 mutation rate is 1.0. The convergence can be achieved and the optimum solution was approached
487 gradually as the mutation rate descends from 1.0 to 0.4. Nevertheless, if the mutation rate is zero,
488 the optimization prematurely ended at the 46th generation without exploring the whole search space.
489 Thus, the mutation probability is recommended to be higher than zero but lower than 0.4 for
490 acquiring a global optimal solution in this case study.

491

492 **4.4.Optimum design configuration under different weather conditions**

493 The selected five cities are all located in hot and humid tropical or subtropical areas with high
494 population densities, where the high-rise residential building format in Hong Kong has a great
495 application potential. As per the comparison conducted in Section 3.1, these cities share common
496 climatic characteristics but differs with each other in terms of average levels and trends of the
497 temperatures, humidity, solar radiation and wind velocity. For the above reason, the optimum design
498 for each city features the following similarities and differences (See Table 3).

499 To minimize the total building energy demand, all optimal solutions are characterized by low
500 window transmittances (close to the lower input limit 0.10), high window U-values (close to the
501 upper input limit 6.00) and high window to ground ratios (close to the upper input limit 0.50). The
502 high window to ground ratio and window U-value help to make full use of natural ventilation and
503 release the heat to the outside environment whenever available. External walls, however, have a
504 broader thermal insulation distribution range from 0.09 to 0.61 m² K/W, which is most sensitive to
505 weather conditions. For instance, the relatively higher thermal resistance for optimum design in
506 BKK might correspond to its highest annual temperature and solar radiation. The major building
507 façade of most optimum designs are oriented to north (between 0 to 14° relative to north) to

508 minimize direct solar radiation. This orientation preference fit in with the findings by Bre et al [84].
509 However, the optimal building orientation for SGP is determined as south because of its special
510 geological location close to the equator. Both external and local shadings are not preferred by
511 optimized designs with a low EOA between 8.91° and 14.00° and OPF between 0.04 and 0.05. Less
512 shadings and obstructions offer better daylight and ventilation access whereas increase solar
513 irradiation on building surfaces. In general, the optimum design under each weather condition
514 shares a similar configuration of passive design strategies. For the corresponding energy demands
515 of optimized design solutions, the electric lighting energy varied little across different cites from
516 14.12 kWh/m^2 to 15.25 kWh/m^2 , while the cooling energy fluctuated in a wider range between
517 18.15 kWh/m^2 and 38.72 kWh/m^2 . This result indicates that weather conditions have non-negligible
518 influences over the optimized passive design configuration especially on building thermal insulation
519 levels. More detailed analyses of the sensitivity to weather conditions will be presented as an
520 independent research topic in future works.

521

522 **5. Conclusions**

523 A holistic design-optimization approach is applied to a passively designed generic building
524 with the mixed-mode ventilation and lighting dimming control in hot and humid areas. Variance-
525 based sensitivity analyses were conducted ahead of the optimization to reduce the search space of
526 the evolutionary algorithm by removing insignificant factors. Time series sensitivity indices for the
527 lighting and cooling energy outputs were presented to reveal their correlations with outdoor thermal
528 and solar radiation conditions. Furthermore, passive architectural parameters were explored by
529 NSGA-II under different optimization settings and weather conditions. The most suitable setting
530 and optimum design for each weather profile were presented and discussed. Main conclusions can
531 be drawn as below:

532 1) The variance-based initial sensitivity analysis thoroughly investigated the whole possible
533 distribution ranges of selected major passive design parameters. The obtained first-order and
534 total-order indices were used to exclude the external wall specific heat and infiltration air mass
535 flow coefficient from the problem space of the subsequent optimization of building energy
536 demands. Among these design strategies, window transmittance properties and external

537 obstruction levels were proved to have greater impact on building energy demands, and
538 therefore should be given the increased weighting in any green building design or assessment
539 guidelines. Correlations between sensitivity indices and external weather conditions can also be
540 identified from the monthly variation of sensitivity indices. Furthermore, these sensitivity
541 indices can also help stakeholders in a building project to prioritize the resource allocation to
542 most influential design factors at the earliest opportunity.

543 2) The NSGA-II based optimization was initially conducted with a benchmarking setting of the
544 population size, crossover rate and mutation probability. The Pareto frontier was obtained
545 within the maximum allowable evaluations and a trade-off was identified between the lighting
546 and cooling energy demand. Among Pareto optimal solutions, the lighting energy demand
547 varies slightly from 13.30 kWh/m² to 14.70 kWh/m² whereas the cooling energy demand
548 changes dramatically from 21.04 kWh/m² to 77.60 kWh/m². Conflicts between two objectives
549 were attributed to the fixed light to solar gain ratio as well as the converse effects from the
550 window to ground ratio, overhang projection ratio and external obstructions. The ultimate
551 optimal solution based on equally weighted objectives achieved a low energy demand of 35.73
552 kWh/m² in Hong Kong. This integrated sensitivity analysis and optimization process can be
553 used to incorporate the passive design approach into green building assessment to determine the
554 optimum performance level for grading scales.

555 3) To find the most appropriate setting of NSGA-II to improve the computation efficiency while
556 keep the optimization productivity, different population sizes, crossover probabilities and
557 mutation rates were examined. A population size of 16, a crossover rate between 0.8 and 1.0, as
558 well as a mutation probability between 0.0 and 0.4 were recommended for this optimization
559 study under the specific control and operation modes. This approach offered a more precise
560 algorithm setting compared with using empirical values suggested by existing literatures.

561 4) In addition, this simulation-based optimization process was applied to four other cities with
562 similar climatic characteristics. As a result, the optimum design under all weather conditions
563 showed similar architectural features of low obstruction levels and window transmittances
564 while high window heat transfer coefficients and solar transmittances. But wall insulation
565 levels showed more diverse distribution due to the difference in outdoor temperature and solar

566 radiation conditions. However, for the limitation of this work, extending the current simulation
567 approach to more diverse climatic zones and detailed building design stages involving
568 additional input variables and evaluation objectives will be carried out in the future.

569

570 **Acknowledgment**

571 The work described in this paper was supported by the Hong Kong PhD Fellowship Scheme,
572 the Construction Industry Council of Hong Kong and the Research Institute for Sustainable Urban
573 Development (RISUD) of The Hong Kong Polytechnic University. Appreciation is also given to the
574 Housing Authority of the Hong Kong SAR Government as well as the Sino Green in Hong Kong
575 Limited for supporting our research project in built environment studies.

576

577 **Nomenclatures**

Abbreviation

AFN	airflow network
ANOVA	analysis of variance
BEAM	building environment assessment method
BO	building orientation
EMSD	electrical and mechanical services department
EOA	external obstruction angle
EOD	external obstruction distance
EOH	external obstruction height
FAST	Fourier amplitude sensitivity test
HVAC	heating ventilation and air conditioning
IAMFC	infiltration air mass flow coefficient
LHS	Latin hypercube sampling
NSGA-II	non-dominated sorting genetic algorithm II
OPF	overhang projection fraction
PRH	public rental housing
SA	sensitivity analysis
SHGC	solar heat gain coefficient
SRC	standardized regression coefficient
SRRC	standardized rank regression coefficient

VLT	visible light transmittance
WGR	window to ground ratio
WSH	wall specific heat
WTR	wall thermal resistance
WU	window U-values

578

579 **References**

- 580 [1] Census and Statistics Department, Hong Kong Energy Statistics Annual Report. 2013.
- 581 [2] Wang Y, Kuckelkorn J, Zhao F-Y, Spliethoff H, Lang W. A state of art of review on interactions
582 between energy performance and indoor environment quality in Passive House buildings.
583 Renewable and Sustainable Energy Reviews. 2017;72:1303-19.
- 584 [3] Chen X, Yang H, Lu L. A comprehensive review on passive design approaches in green building
585 rating tools. Renewable and Sustainable Energy Reviews. 2015;50:1425-36.
- 586 [4] EMSD. Hong Kong Energy End-use Data 2015. Electrical & Mechanical Services Department.
587 <http://www.emsd.gov.hk>.
- 588 [5] Attia S, Gratia E, De Herde A, Hensen JLM. Simulation-based decision support tool for early
589 stages of zero-energy building design. Energy and Buildings. 2012;49:2-15.
- 590 [6] Chan ALS. Investigation on the appropriate floor level of residential building for installing
591 balcony, from a view point of energy and environmental performance. A case study in
592 subtropical Hong Kong. Energy. 2015;85:620-34.
- 593 [7] Gao CF, Lee WL. Evaluating the influence of openings configuration on natural ventilation
594 performance of residential units in Hong Kong. Building and Environment. 2011;46:961-9.
- 595 [8] Premrov M, Žegarac Leskovar V, Mihalič K. Influence of the building shape on the energy
596 performance of timber-glass buildings in different climatic conditions. Energy. 2016;108:201-
597 11.
- 598 [9] Ochs F, Dermentzis G, Feist W. Minimization of the Residual Energy Demand of Multi-storey
599 Passive Houses – Energetic and Economic Analysis of Solar Thermal and PV in Combination
600 with a Heat Pump. Energy Procedia. 2014;48:1124-33.
- 601 [10] Tian W. A review of sensitivity analysis methods in building energy analysis. Renewable and
602 Sustainable Energy Reviews. 2013;20:411-9.
- 603 [11] Sun Y. Sensitivity analysis of macro-parameters in the system design of net zero energy
604 building. Energy and Buildings. 2015;86:464-77.
- 605 [12] Lam JC, Hui SCM. Sensitivity analysis of energy performance of office buildings. Building
606 and Environment. 1996;31:27-39.
- 607 [13] Raji B, Tenpierik MJ, van den Dobbelen A. An assessment of energy-saving solutions for
608 the envelope design of high-rise buildings in temperate climates: A case study in the
609 Netherlands. Energy and Buildings. 2016;124:210-21.
- 610 [14] Samuelson H, Claussnitzer S, Goyal A, Chen Y, Romo-Castillo A. Parametric energy
611 simulation in early design: High-rise residential buildings in urban contexts. Building and
612 Environment. 2016;101:19-31.
- 613 [15] Zhao M, Künzle HM, Antretter F. Parameters influencing the energy performance of residential
614 buildings in different Chinese climate zones. Energy and Buildings. 2015;96:64-75.

- 615 [16] Lam JC, Li DHW. An analysis of daylighting and solar heat for cooling-dominated office
616 buildings. *Solar Energy*. 1999;65:251-62.
- 617 [17] Park B, Srubar Iii WV, Krarti M. Energy performance analysis of variable thermal resistance
618 envelopes in residential buildings. *Energy and Buildings*. 2015;103:317-25.
- 619 [18] Blight TS, Coley DA. Sensitivity analysis of the effect of occupant behaviour on the energy
620 consumption of passive house dwellings. *Energy and Buildings*. 2013;66:183-92.
- 621 [19] Menberg K, Heo Y, Choudhary R. Sensitivity analysis methods for building energy models:
622 Comparing computational costs and extractable information. *Energy and Buildings*.
623 2016;133:433-45.
- 624 [20] Tian W, Liu Y, Heo Y, Yan D, Li Z, An J, et al. Relative importance of factors influencing
625 building energy in urban environment. *Energy*. 2016;111:237-50.
- 626 [21] Breesch H, Janssens A. Performance evaluation of passive cooling in office buildings based on
627 uncertainty and sensitivity analysis. *Solar Energy*. 2010;84:1453-67.
- 628 [22] Yıldız Y, Arsan ZD. Identification of the building parameters that influence heating and cooling
629 energy loads for apartment buildings in hot-humid climates. *Energy*. 2011;36:4287-96.
- 630 [23] Silva AS, Almeida LSS, Ghisi E. Decision-making process for improving thermal and energy
631 performance of residential buildings: A case study of constructive systems in Brazil. *Energy and*
632 *Buildings*. 2016;128:270-86.
- 633 [24] Rocha APdA, Goffart J, Houben L, Mendes N. On the uncertainty assessment of incident direct
634 solar radiation on building facades due to shading devices. *Energy and Buildings*.
635 2016;133:295-304.
- 636 [25] Li Y, Yu W, Li B, Yao R. A multidimensional model for green building assessment: A case
637 study of a highest-rated project in Chongqing. *Energy and Buildings*. 2016;125:231-43.
- 638 [26] GhaffarianHoseini A, Dahlan ND, Berardi U, GhaffarianHoseini A, Makaremi N,
639 GhaffarianHoseini M. Sustainable energy performances of green buildings: A review of current
640 theories, implementations and challenges. *Renewable and Sustainable Energy Reviews*.
641 2013;25:1-17.
- 642 [27] Ortiz J, Fonseca A, Salom J, Garrido N, Fonseca P, Russo V. Comfort and economic criteria for
643 selecting passive measures for the energy refurbishment of residential buildings in Catalonia.
644 *Energy and Buildings*. 2016;110:195-210.
- 645 [28] Carlucci S, Cattarin G, Causone F, Pagliano L. Multi-objective optimization of a nearly zero-
646 energy building based on thermal and visual discomfort minimization using a non-dominated
647 sorting genetic algorithm (NSGA-II). *Energy and Buildings*. 2015;104:378-94.
- 648 [29] Futrell BJ, Ozelkan EC, Brentrup D. Bi-objective optimization of building enclosure design for
649 thermal and lighting performance. *Building and Environment*. 2015;92:591-602.
- 650 [30] Lin B, Yu Q, Li Z, Zhou X. Research on parametric design method for energy efficiency of
651 green building in architectural scheme phase. *Frontiers of Architectural Research*. 2013;2:11-22.
- 652 [31] Mangkuto RA, Rohmah M, Asri AD. Design optimisation for window size, orientation, and
653 wall reflectance with regard to various daylight metrics and lighting energy demand: A case
654 study of buildings in the tropics. *Applied Energy*. 2016;164:211-9.
- 655 [32] Konis K, Gamas A, Kensek K. Passive performance and building form: An optimization
656 framework for early-stage design support. *Solar Energy*. 2016;125:161-79.
- 657 [33] Negendahl K, Nielsen TR. Building energy optimization in the early design stages: A
658 simplified method. *Energy and Buildings*. 2015;105:88-99.

- 659 [34] Xu W, Chong A, Karaguzel OT, Lam KP. Improving evolutionary algorithm performance for
660 integer type multi-objective building system design optimization. *Energy and Buildings*.
661 2016;127:714-29.
- 662 [35] Zhang L, Zhang L, Wang Y. Shape optimization of free-form buildings based on solar radiation
663 gain and space efficiency using a multi-objective genetic algorithm in the severe cold zones of
664 China. *Solar Energy*. 2016;132:38-50.
- 665 [36] Delgarm N, Sajadi B, Kowsary F, Delgarm S. Multi-objective optimization of the building
666 energy performance: A simulation-based approach by means of particle swarm optimization
667 (PSO). *Applied Energy*. 2016;170:293-303.
- 668 [37] Si B, Tian Z, Jin X, Zhou X, Tang P, Shi X. Performance indices and evaluation of algorithms
669 in building energy efficient design optimization. *Energy*. 2016;114:100-12.
- 670 [38] Chen X, Yang H, Sun K. A holistic passive design approach to optimize indoor environmental
671 quality of a typical residential building in Hong Kong. *Energy*. 2016;113:267-81.
- 672 [39] Chen X, Yang H, Sun K. Developing a meta-model for sensitivity analyses and prediction of
673 building performance for passively designed high-rise residential buildings. *Applied Energy*.
- 674 [40] Chen X, Yang H. Combined thermal and daylight analysis of a typical public rental housing
675 development to fulfil green building guidance in Hong Kong. *Energy and Buildings*.
676 2015;108:420-32.
- 677 [41] Lam JC. Residential sector air conditioning loads and electricity use in Hong Kong. *Energy*
678 *Conversion and Management*. 2000;41:1757-68.
- 679 [42] Lam JC, Tang HL, Li DHW. Seasonal variations in residential and commercial sector
680 electricity consumption in Hong Kong. *Energy*. 2008;33:513-23.
- 681 [43] Chen X, Yang H, Wang Y. Parametric study of passive design strategies for high-rise residential
682 buildings in hot and humid climates: miscellaneous impact factors. *Renewable and Sustainable*
683 *Energy Reviews*. 2017;69:442-60.
- 684 [44] Niachou K, Hassid S, Santamouris M, Livada I. Comparative monitoring of natural, hybrid and
685 mechanical ventilation systems in urban canyons. *Energy and Buildings*. 2005;37:503-13.
- 686 [45] Strømmand-Andersen J, Sattrup PA. The urban canyon and building energy use: Urban density
687 versus daylight and passive solar gains. *Energy and Buildings*. 2011;43:2011-20.
- 688 [46] Allegrini J, Dorer V, Carmeliet J. Impact of radiation exchange between buildings in urban
689 street canyons on space cooling demands of buildings. *Energy and Buildings*. 2016;127:1074-
690 84.
- 691 [47] Mavromatidis LE, Marsault X, Lequay H. Daylight factor estimation at an early design stage to
692 reduce buildings' energy consumption due to artificial lighting: A numerical approach based on
693 Doehlert and Box–Behnken designs. *Energy*. 2014;65:488-502.
- 694 [48] Li DHW, Wong SL, Tsang CL, Cheung GHW. A study of the daylighting performance and
695 energy use in heavily obstructed residential buildings via computer simulation techniques.
696 *Energy and Buildings* 2006. p. 1343-8.
- 697 [49] Wang Z, Yang L. Delinking indicators on regional industry development and carbon emissions:
698 Beijing–Tianjin–Hebei economic band case. *Ecological Indicators*. 2015;48:41-8.
- 699 [50] BEAM. BEAM Plus New Buildings Version 1.2. HKGBC and BEAM Society Limited. 2012.
- 700 [51] ENERGYPLUS™. Basic Concepts Manual - Essential Information You Need about Running
701 EnergyPlus: US Department of Energy; 2013.
- 702 [52] ENERGYPLUS™. EnergyPlus Engineering Reference - The Reference to EnergyPlus

703 Calculations: US Department of Energy; 2013.

704 [53] Fang YP, Hyde TJ, Arya F, Hewitt N, Wang RZ, Dai YJ. Enhancing the thermal performance of
705 triple vacuum glazing with low-emittance coatings. *Energy and Buildings*. 2015;97:186-95.

706 [54] Mechri HE, Capozzoli A, Corrado V. USE of the ANOVA approach for sensitive building
707 energy design. *Applied Energy*. 2010;87:3073-83.

708 [55] Al-Obaidi KM, Ismail M, Abdul Rahman AM. Passive cooling techniques through reflective
709 and radiative roofs in tropical houses in Southeast Asia: A literature review. *Frontiers of
710 Architectural Research*. 2014;3:283-97.

711 [56] Ozel M. The influence of exterior surface solar absorptivity on thermal characteristics and
712 optimum insulation thickness. *Renewable Energy*. 2012;39:347-55.

713 [57] Census and Statistics Department, Population by type of housing. 2007.

714 [58] Chen X, Yang H, Sun K. Developing a meta-model for sensitivity analyses and prediction of
715 building performance for passively designed high-rise residential buildings. *Applied Energy*.
716 2017;194:422-39.

717 [59] Zhai Z, Johnson M-H, Krarti M. Assessment of natural and hybrid ventilation models in
718 whole-building energy simulations. *Energy and Buildings*. 2011;43:2251-61.

719 [60] Schulze T, Eicker U. Controlled natural ventilation for energy efficient buildings. *Energy and
720 Buildings*. 2013;56:221-32.

721 [61] CIBSE. Code for Lighting. Chartered Institution of Building Services Engineers, London;
722 2002.

723 [62] Chen X, Yang H, Zhang W. A comprehensive sensitivity study of major passive design
724 parameters for the public rental housing development in Hong Kong. *Energy*. 2015;93:1804-18.

725 [63] Rupp RF, Ghisi E. What is the most adequate method to assess thermal comfort in hybrid
726 commercial buildings located in hot-humid summer climate? *Renewable and Sustainable
727 Energy Reviews*. 2014;29:449-62.

728 [64] Sorgato MJ, Melo AP, Lamberts R. The effect of window opening ventilation control on
729 residential building energy consumption. *Energy and Buildings*. 2016;133:1-13.

730 [65] de Dear RJ, Brager GS. Thermal comfort in naturally ventilated buildings: revisions to
731 ASHRAE Standard 55. *Energy and Buildings*. 2002;34:549-61.

732 [66] Luo M, Cao B, Damiens J, Lin B, Zhu Y. Evaluating thermal comfort in mixed-mode
733 buildings: A field study in a subtropical climate. *Building and Environment*. 2015;88:46-54.

734 [67] Zhong K, Fu H, Kang Y, Peng X. Indoor thermal conditions and the potential of energy
735 conservation of naturally ventilated rooms in summer, China. *Energy and Buildings*.
736 2012;55:183-8.

737 [68] Goto T, Mitamura T, Yoshino H, Tamura A, Inomata E. Long-term field survey on thermal
738 adaptation in office buildings in Japan. *Building and Environment*. 2007;42:3944-54.

739 [69] James G, Witten D, Hastie T, Tibshirani R. An Introduction to Statistical Learning with
740 Application in R: Springer; 2013.

741 [70] Giap GE, Kosuke N. Sensitivity Analysis Using Sobol 'Variance-Based Method on the
742 Haverkamp Constitutive Functions Implemented in Richards' Water Flow Equation. *Malaysian
743 Journal of Soil Science*. 2014;18:19-33.

744 [71] A. Saltelli MR, Terry Andres, Francesca Campolongo, Jessica Cariboni, Debora Gatelli,
745 Michaela Saisana, Stefano Tarantola. *Global Sensitivity Analysis: The Primer*: John Wiley &
746 Sons Ltd; 2008.

- 747 [72] Mara TA, Tarantola S. Application of global sensitivity analysis of model output to building
748 thermal simulations. *Building Simulation*. 2008;1:290-302.
- 749 [73] Qian J. *Towards a Whole-life Value Optimisation Model for Facade Design*: University of
750 Cambridge; 2013.
- 751 [74] Wu H. *A multi-objective optimization model for green building design*: The University of
752 Hong Kong (Pokfulam, Hong Kong); 2012.
- 753 [75] Zhang Y. Use jEPlus as an efficient building design optimization tool. CIBSE ASHRAE
754 Technical Symposium, Imperial College, London UK – 18 and 19 April, 2012, London.
- 755 [76] Hamdy M, Nguyen A-T, Hensen JLM. A performance comparison of multi-objective
756 optimization algorithms for solving nearly-zero-energy-building design problems. *Energy and*
757 *Buildings*. 2016;121:57-71.
- 758 [77] Khoroshiltseva M, Slanzi D, Poli I. A Pareto-based multi-objective optimization algorithm to
759 design energy-efficient shading devices. *Applied Energy*.
- 760 [78] Weise T. *Global Optimization Algorithms – Theory and Application*: <http://www.it-weise.de>;
761 2009.
- 762 [79] Chen X, Yang H. An Exhaustive Parametric Study on Major Passive Design Strategies of a
763 Typical High-rise Residential Building in Hong Kong. *Energy Procedia*. 2016;88:748-53.
- 764 [80] Kristensen MH, Petersen S. Choosing the appropriate sensitivity analysis method for building
765 energy model-based investigations. *Energy and Buildings*. 2016;130:166-76.
- 766 [81] Martinez NA. Solving the Black Box: Inverse Approach for Ideal Building Dynamic Behaviour
767 Using Multi-Objective Optimization with Energyplus. 8th Windsor Conference: Counting the
768 cost of comfort in a changing world. Cumberland Lodge, Windsor, UK, 10-13 April 2014.
769 London: Network for Comfort and Energy Use in Buildings2014.
- 770 [82] Spaho E, Oda T, Barolli A, Xhafa F, Barolli L, Takizawa M. A Comparison Study for Different
771 Settings of Crossover and Mutation Rates Using WMN-GA Simulation System. In: J. Park J,
772 Chao H-C, S. Obaidat M, Kim J, editors. *Computer Science and Convergence: CSA 2011 &*
773 *WCC 2011 Proceedings*. Dordrecht: Springer Netherlands; 2012. p. 643-50.
- 774 [83] Lin W-Y, Lee W-Y, Hong T-P. Adapting Crossover and Mutation Rates in Genetic Algorithms.
775 *J Inf Sci Eng*. 2003;19:889-903.
- 776 [84] Bre F, Silva AS, Ghisi E, Fachinotti VD. Residential building design optimisation using
777 sensitivity analysis and genetic algorithm. *Energy and Buildings*. 2016;133:853-66.
- 778
- 779

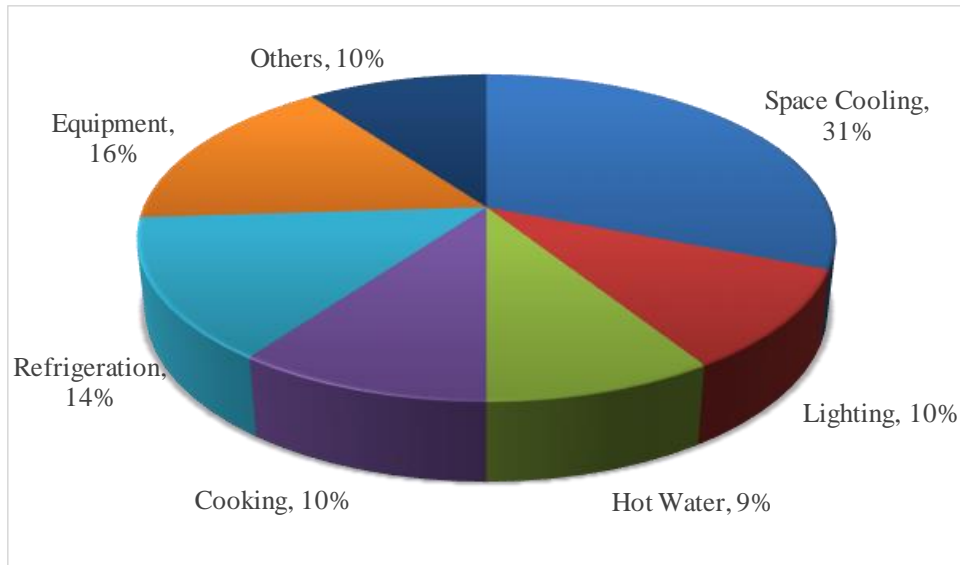


Fig. 1 Energy end use statistics of residential buildings in Hong Kong (by EMSD)

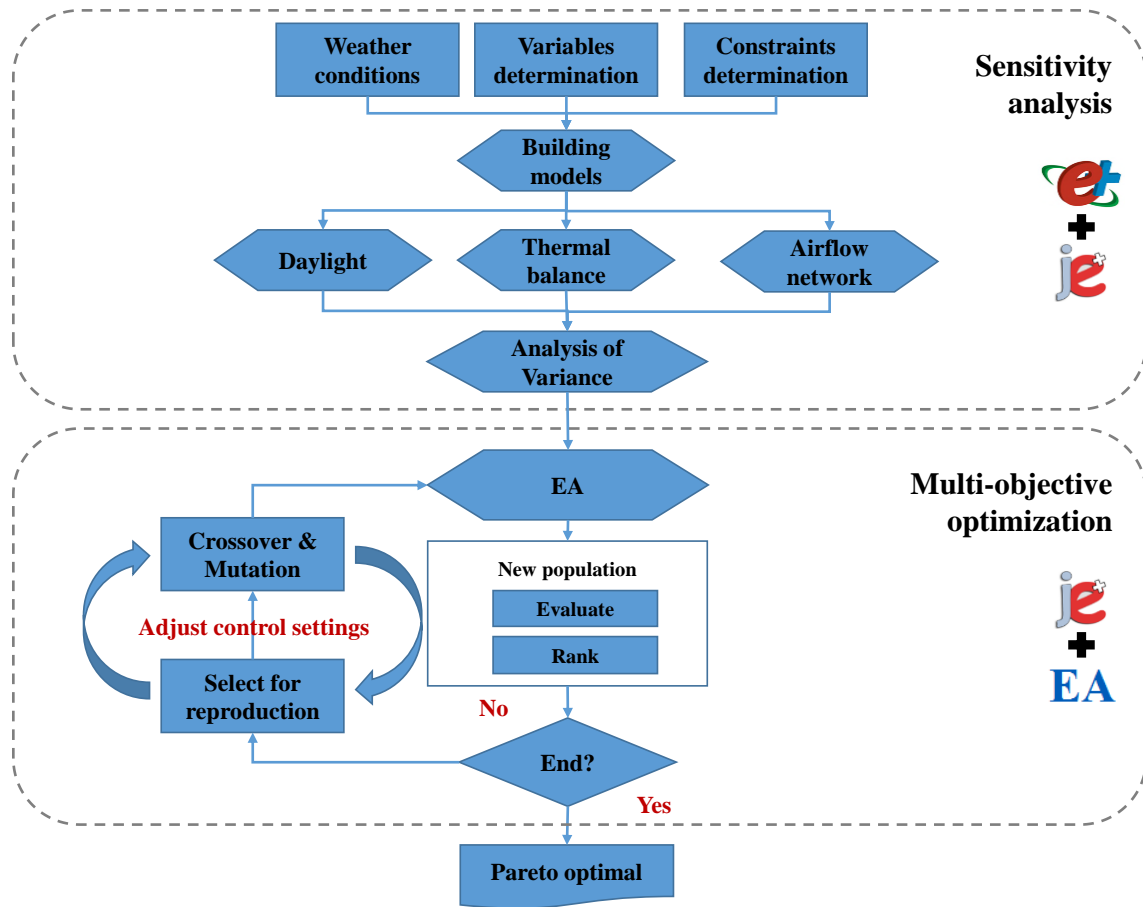
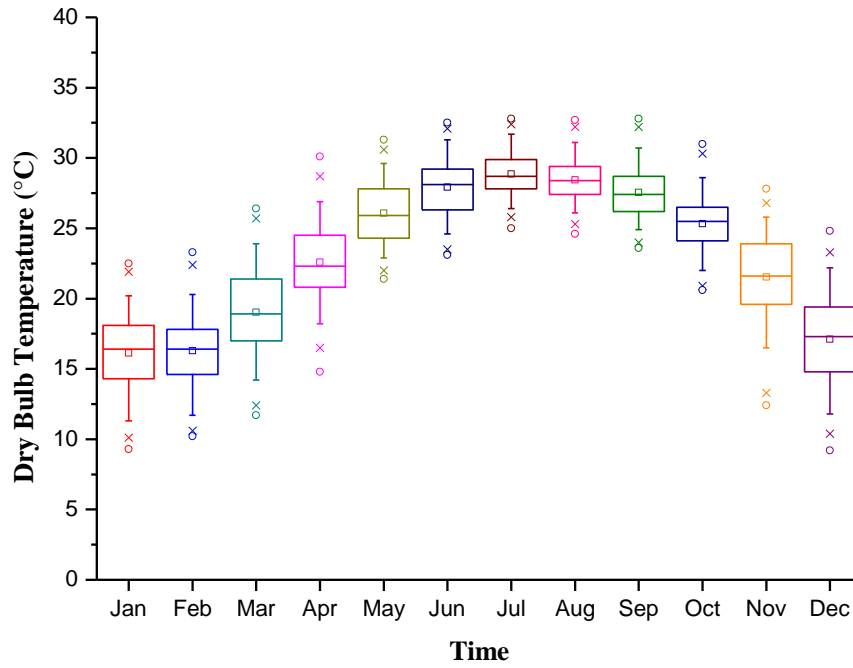
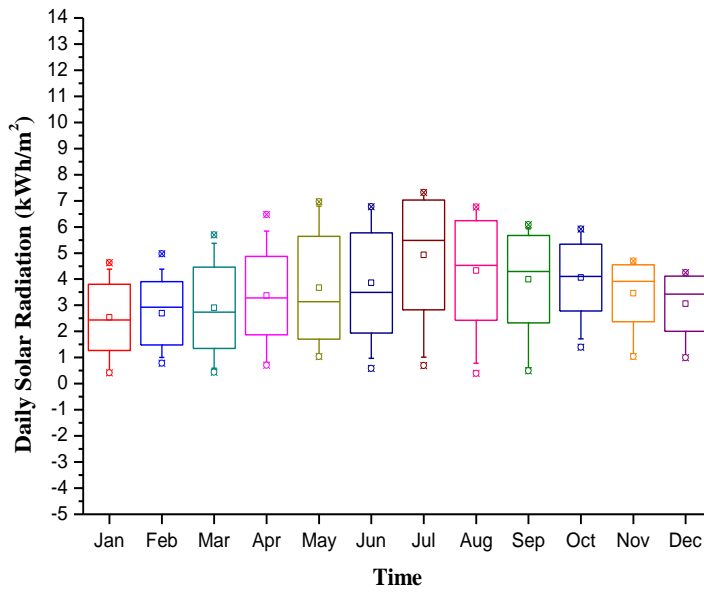


Fig. 2 Proposed flowchart of research methodology



a. Hourly dry bulb temperature



b. Daily solar radiation

Fig. 3 Weather conditions of Hong Kong

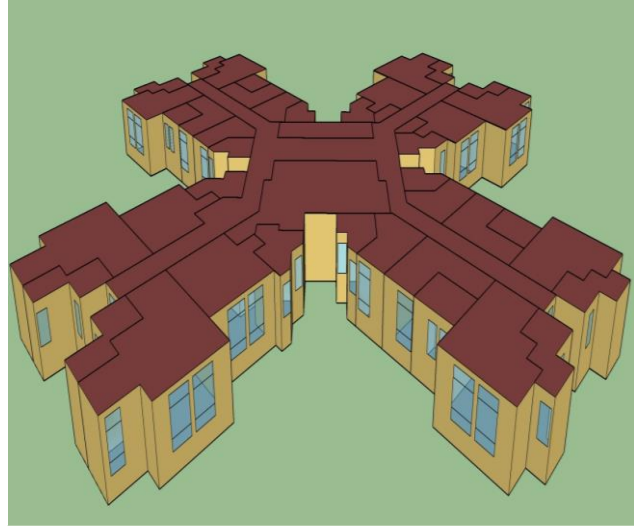
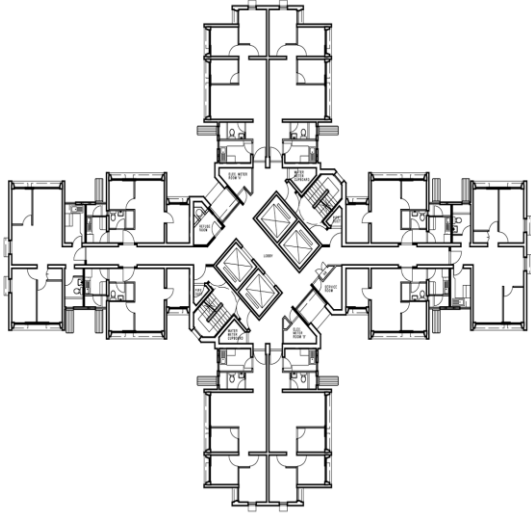


Fig. 4 Typical floor plan and model in the simulation environment

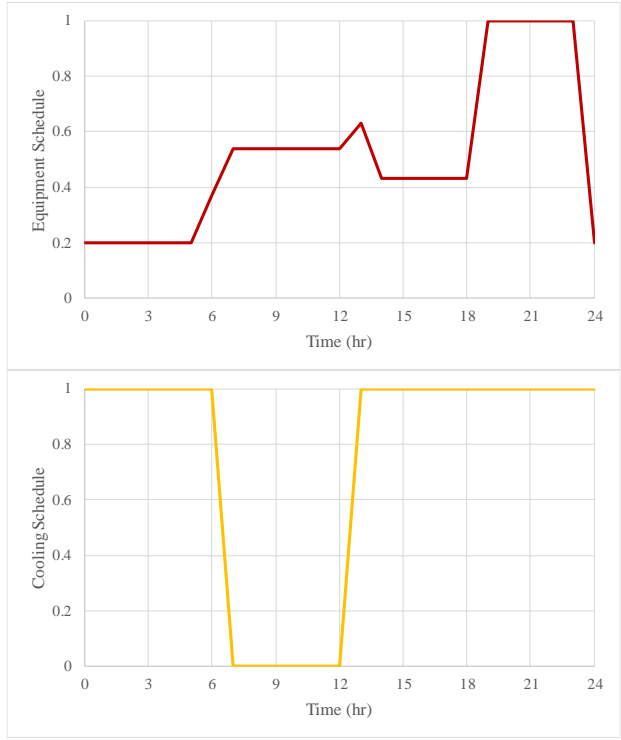
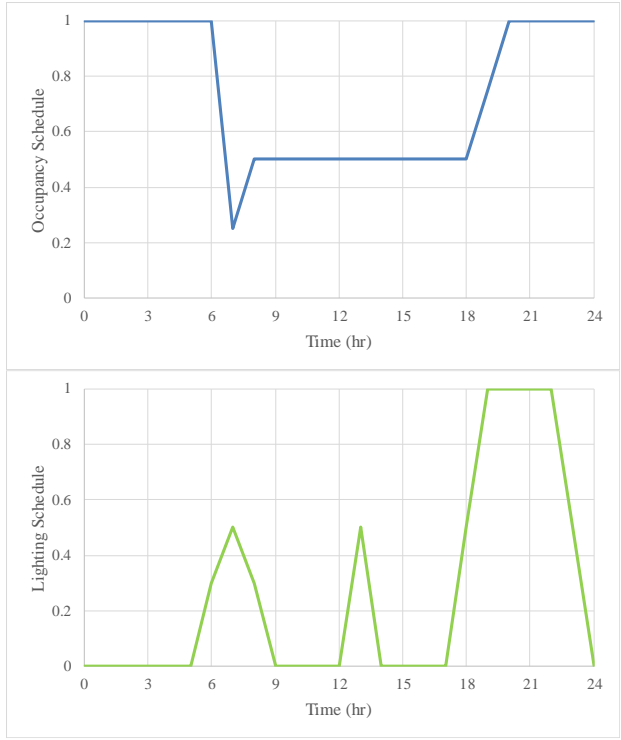


Fig. 5 Building operation schedules

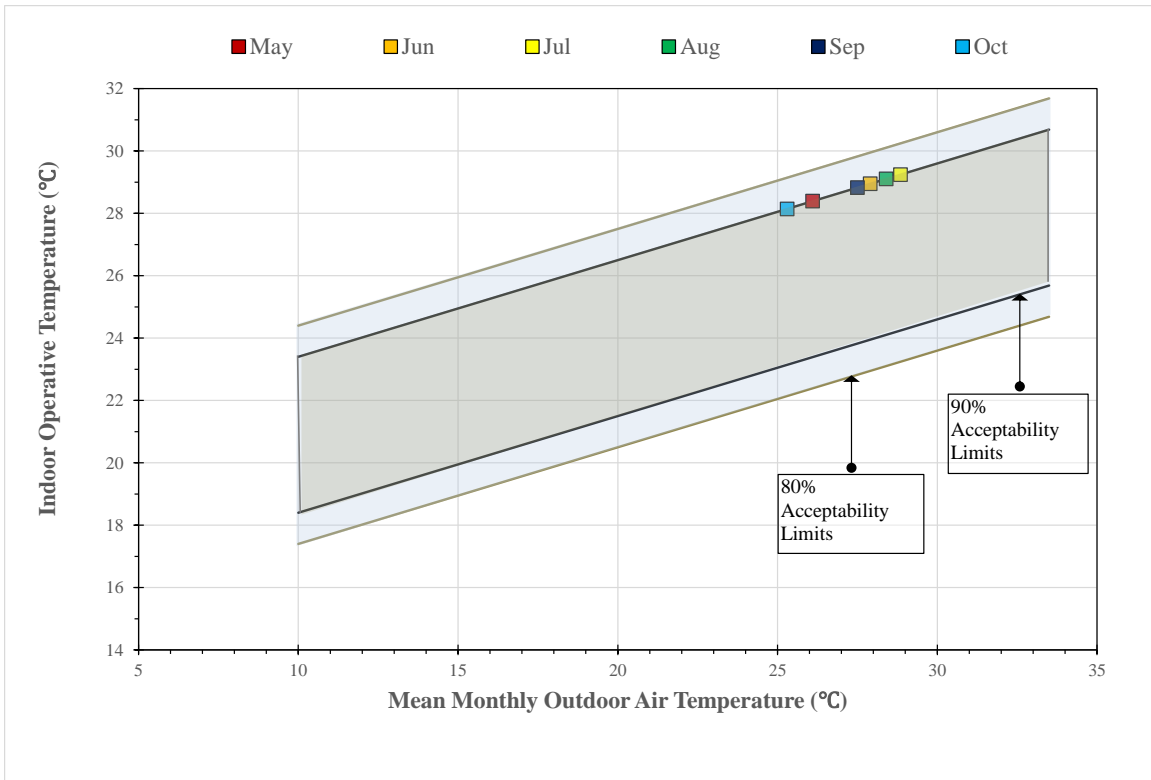


Fig. 6 Monthly cooling temperature setpoints according to the ASHARE 55 adaptive comfort model

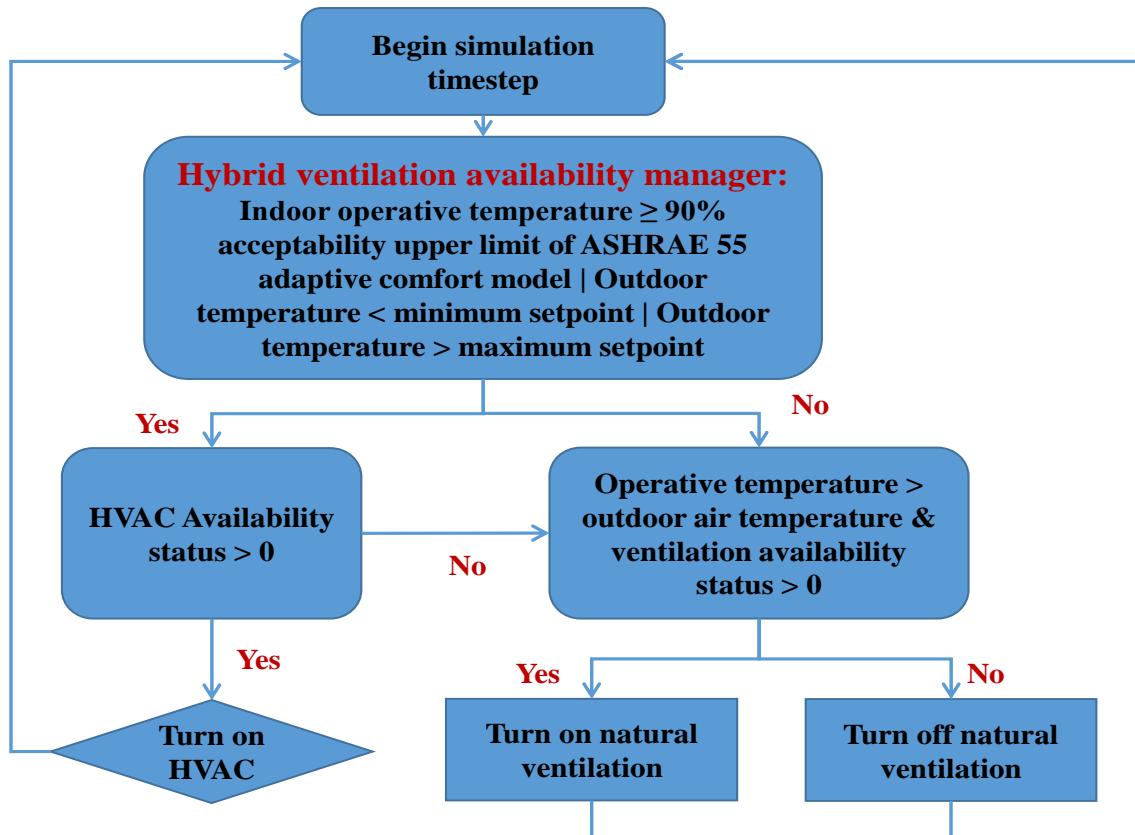


Fig. 7 The hybrid ventilation operation flowchart

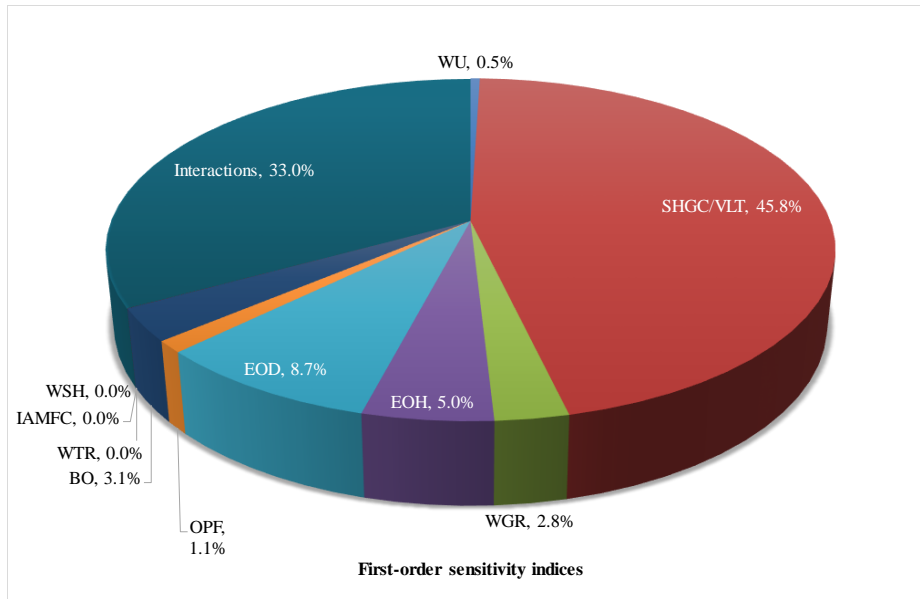


Fig. 8 First-order sensitivity indices by FAST

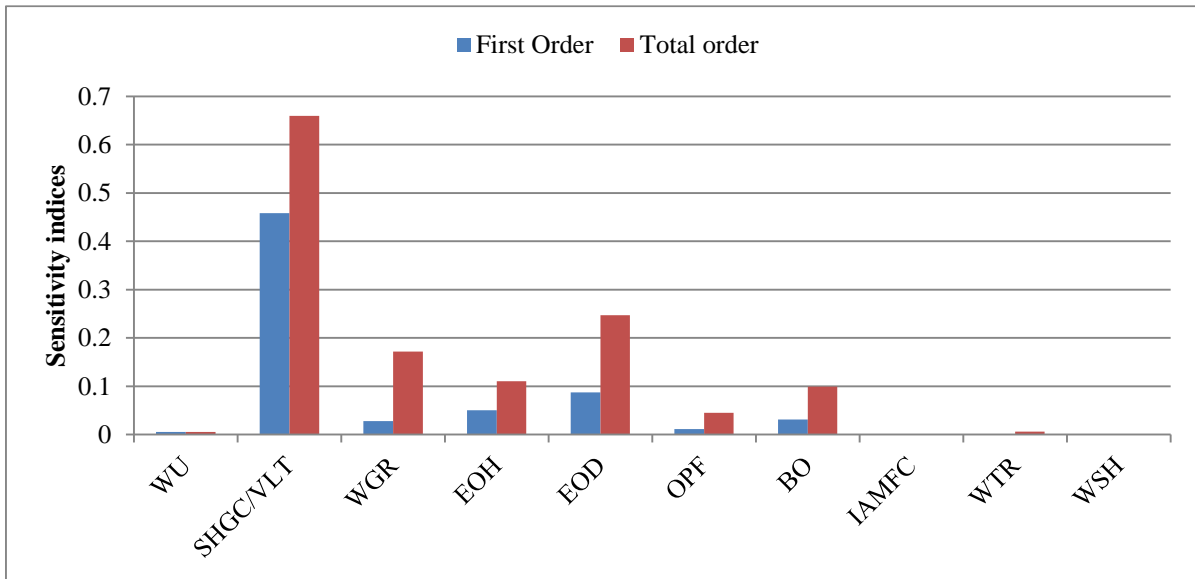


Fig. 9 The comparison of fist-order and total-order indices

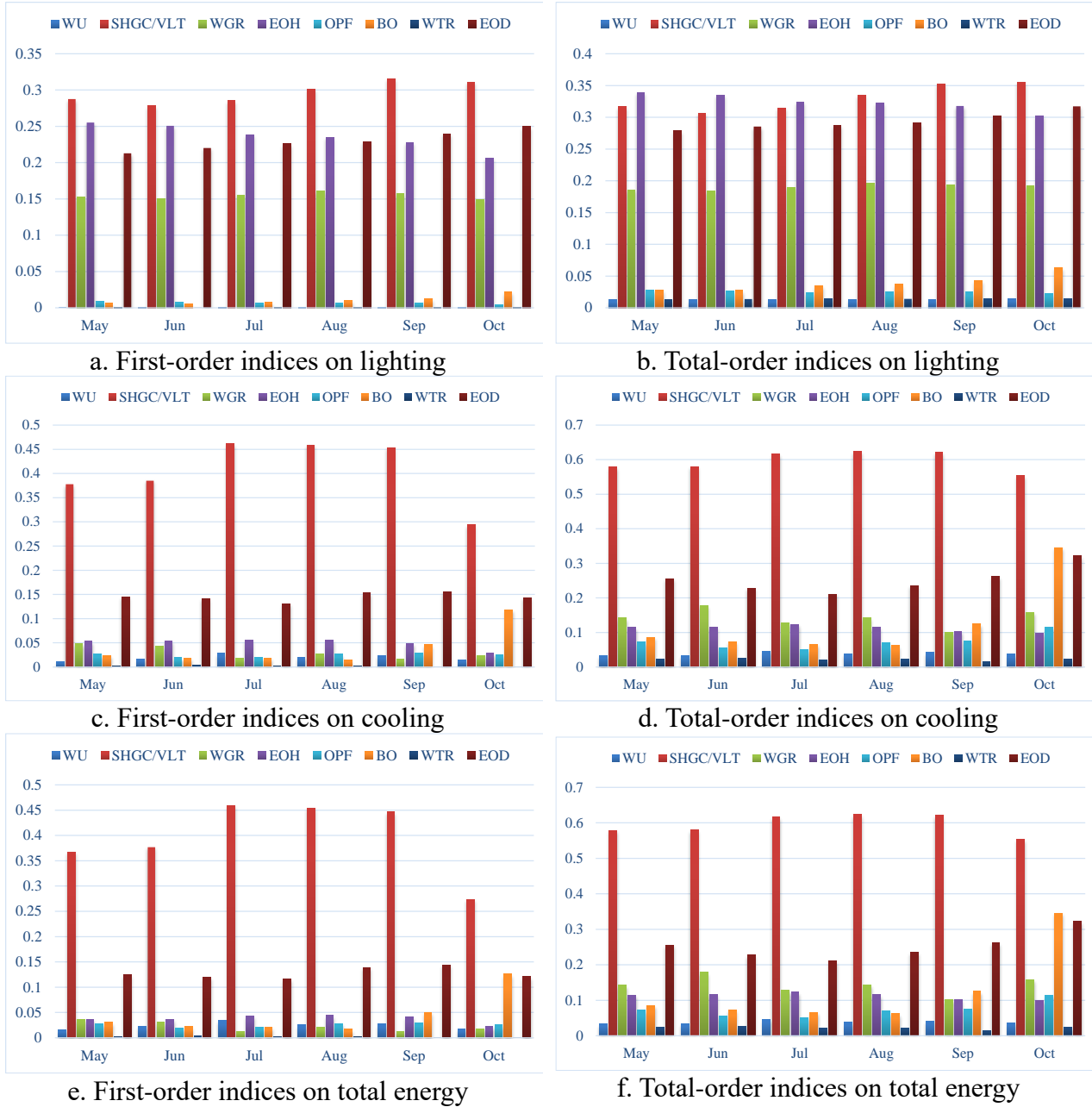


Fig. 10 Sensitivity monthly profile for the output of cooling, lighting and total energy

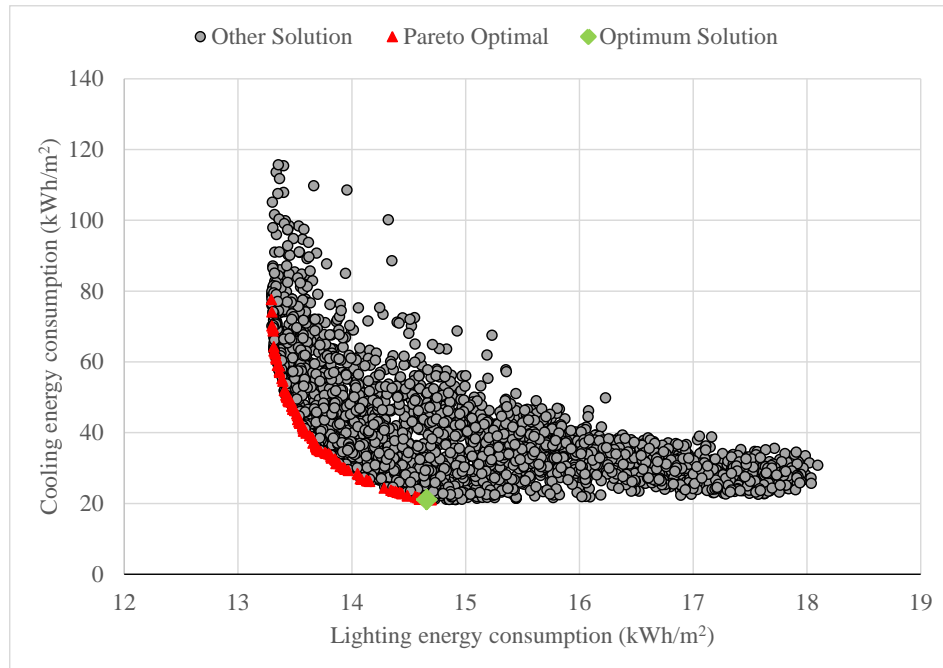
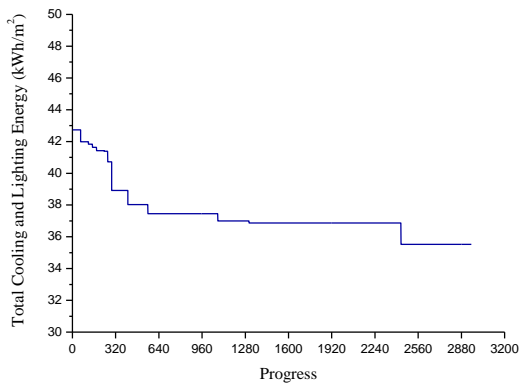
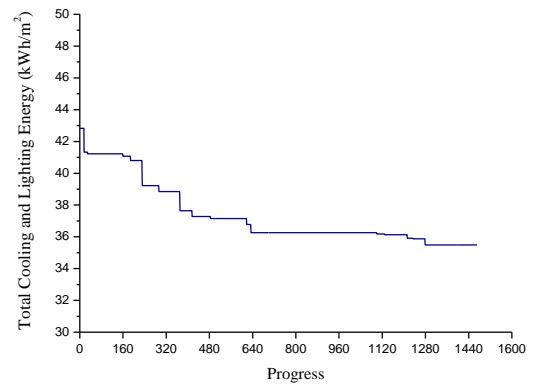


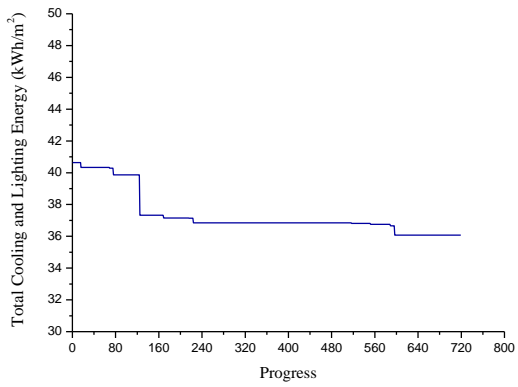
Fig. 11 Distribution of the Pareto frontier and optimum solution between the lighting and cooling energy consumption



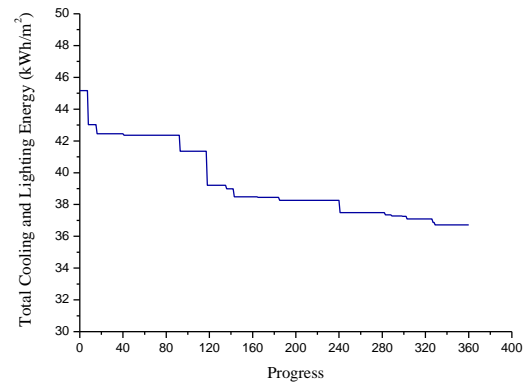
a. Population size = 32



b. Population size = 16

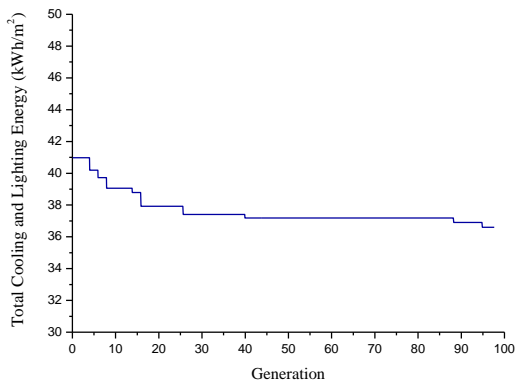


c. Population size = 8

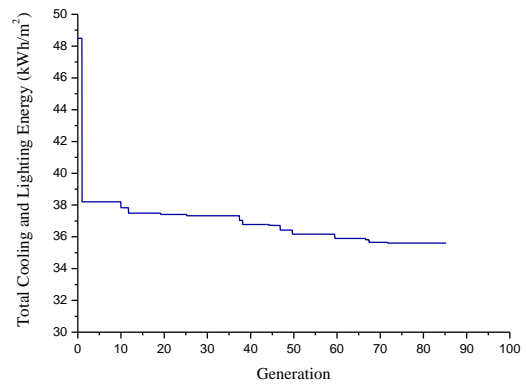


d. Population size = 4

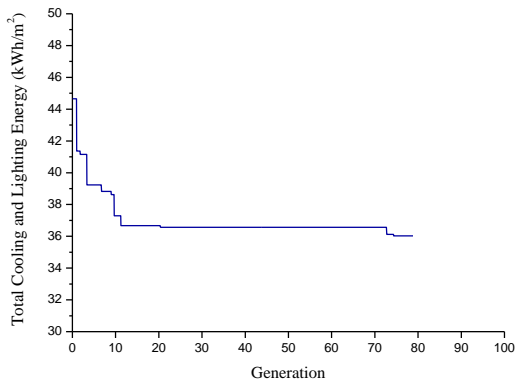
Fig. 12 The convergence progresses under different population size



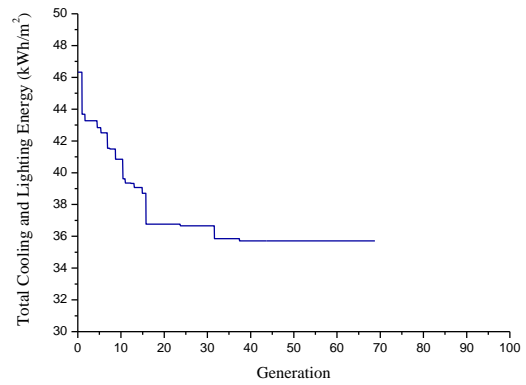
a. Crossover probability = 1.0



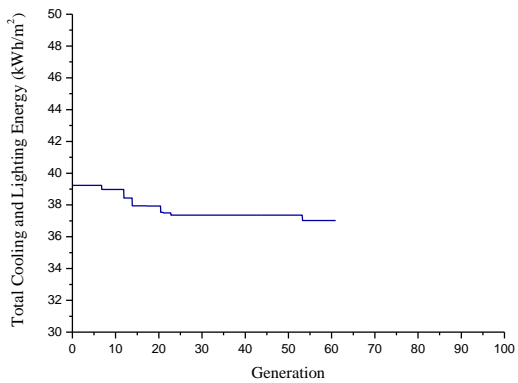
b. Crossover probability = 0.8



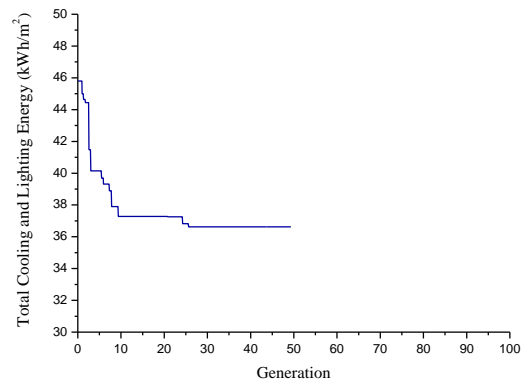
c. Crossover probability = 0.6



d. Crossover probability = 0.4

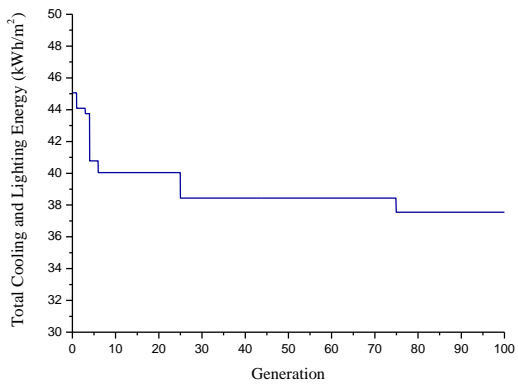


e. Crossover probability = 0.2

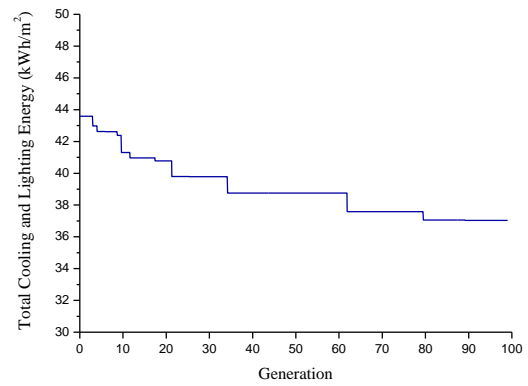


f. Crossover probability = 0.0

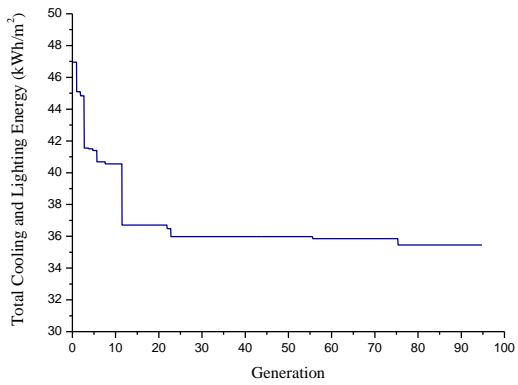
Fig. 13 The convergence progresses under different crossover probability



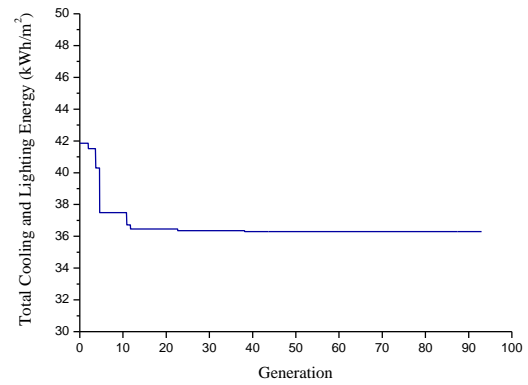
a. Mutation probability = 1.0



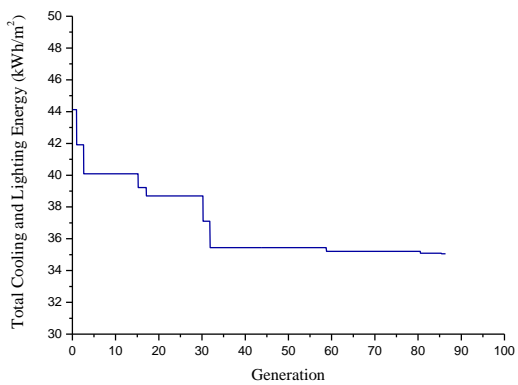
b. Mutation probability = 0.8



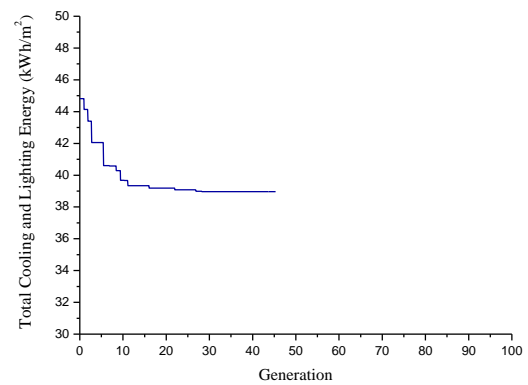
c. Mutation probability = 0.6



d. Mutation probability = 0.4



e. Mutation probability = 0.2



f. Mutation probability = 0.0

Fig. 14 The convergence progresses under different mutation probability

Table 1 General information of five selected representative cities

	Lat. (°)	Long. (°)	Elev. (m)	HDD	CDD
Hong Kong (HK)	22.33	114.17	62	237	1976
Guangzhou (GZ)	23.17	113.33	42	402	2036
Taipei (TPE)	25.07	121.55	6	242	2022
Bangkok (BKK)	13.73	100.57	4	0	3873
Singapore (SGP)	1.37	103.98	16	0	3537

HDD and CDD: Annual heating and cooling degree-days, base 18.3°C

Table 2 Summary of research on simulation-based passive design approach

Category of references	Reference indices
1. Local sensitivity analysis	[10], [11], [12], [13], [14], [15], [16], [17], [18]
2. Global sensitivity analysis (multi-method)	[19], [20]
2.1. Regression method	[21], [22]
2.2. Variance-based method	[24]
2.3. Screening-based method	[23]
3. Multi-objective Optimization (multi-method)	[37]
3.1. Evolutionary Algorithm	[27], [28], [30], [33], [34], [35]
3.2. Swarm Intelligence	[29], [32], [36]
4. Optimization with sensitivity analysis	[31] (Regression method)

Table 3 Optimum design conditions for five cities

	HK	TPE	GZ	SGP	BKK
WU (W/m ² ·K)	5.81	5.87	5.27	5.67	5.82
SHGC/VLT (-)	0.11	0.10	0.11	0.11	0.10
EOA (°)	14.00	10.00	10.07	8.91	10.85
WGR (-)	0.49	0.50	0.50	0.49	0.50
OPF (-)	0.15	0.04	0.14	0.10	0.15
BO (°)	5.00	3.00	14.00	174.00	359.00
WTR (m ² ·K/W)	0.26	0.14	0.09	0.11	0.61
Lighting (kWh/m ²)	14.66	14.12	14.83	15.25	14.39
Cooling (kWh/m ²)	21.07	18.15	18.98	21.86	38.72
Total (kWh/m ²)	35.73	32.27	33.81	37.11	53.11